



Label-free potentiometric aptasensing platform for the detection of Pb^{2+} based on guanine quadruplex structure

Wanxin Tang^a, Juan Yu^a, Zhenzhen Wang^a, Itthipon Jeerapan^b, Lu Yin^c, Fan Zhang^{a,*}, Pingang He^{a,**}

^a School of Chemistry and Molecular Engineering, East China Normal University, 500 Dongchuan Road, Shanghai, 200241, PR China

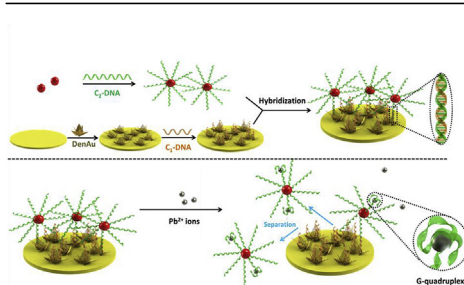
^b Department of Chemistry, Faculty of Science, Prince of Songkla University, Hat Yai, Songkla 90112, Thailand

^c Department of NanoEngineering, University of California, San Diego La Jolla, CA, 92093, USA

HIGHLIGHTS

- A stable and selective potentiometric aptasensor for the detection of lead ions.
- Applying a potentiometric method together with gold dendritic to detect small ions species.
- Low-cost and low-power consumption design for label-free potentiometric aptasensor.

GRAPHICAL ABSTRACT



ARTICLE INFO

Article history:

Received 15 March 2019

Received in revised form

21 May 2019

Accepted 10 June 2019

Available online 14 June 2019

Keywords:

Potentiometry

Aptasensors

Gold dendritic

G-quadruplex

Pb^{2+}

ABSTRACT

Potentiometric aptasensors enhanced by integrating advanced nanomaterials are of particular interest for the detection of multiplex species (e.g., proteins, bacteria, micro-organisms) due to their low cost, ease of operation, and low detection limits. However, potentiometric detection of small ionic species aptasensors is still challenging. This article describes the first example of a label-free G-quadruplex-based potentiometric aptasensing platform for the detection of Pb^{2+} . Polyion oligonucleotide-labeled gold nanoparticles (AuNPs-DNA) as probes are modified on Au electrode, providing high-density negative charge on the electrode surface. These signal-amplifying probes can selectively form G-quadruplexes with the presence of Pb^{2+} ions and reduce the negative charges on the electrode surface, hence achieving potentiometric detection of Pb^{2+} ions with high selectivity. The AuNPs-DNA-based aptasensor shows an acceptable sensitivity over a wide range from 10^{-11} to 10^{-6} M with a detection limit of 8.5 pM. Furthermore, confirmed by coupled plasma mass spectrometry, the sensing platform is capable of performing effective and accurate detection of Pb^{2+} level in real water samples. The presented aptasensor offers a fast, convenient, low-maintenance, and highly sensitive alternative for on-site water pollution detections.

© 2019 Elsevier B.V. All rights reserved.

1. Introduction

Solid-state ion-selective electrodes (ISEs) have been regarded as important sensing components for ionic species, especially for

* Corresponding author.

** Corresponding author.

E-mail addresses: fzhang@chem.ecnu.edu.cn (F. Zhang), pghe@chem.ecnu.edu.cn (P. He).

heavy metal ions [1–5], for their advantages of low power consumption, robust construction, and ease of miniaturization [6–8]. Heavy metal ions such as lead ions (Pb^{2+}) are nonbiodegradable, highly toxic, and can accumulate and induce adverse effects in the human body upon trace amount of exposure [9,10]. Solvent polymeric membranes containing neutral or charged carriers (ionophores) have been widely applied to solid-state ISEs for the detection of heavy metals [11–13]. Researchers have put tremendous efforts to improve the stability and sensitivity of solid-state ISEs by introducing different synthetic receptors, and using conductive polymers and nanomaterials as the ion-to-electron transducers [14–16]. Nevertheless, the detection of various types of heavy metal ions using polymeric-membranes-based solid-state ISEs is still facing challenges such as limited detection limits and component leaching from the ion selective membranes (ISMs). To date, there are few reports on polymeric membranes based solid-state ISE, which encourages the development of a new receptor-based potentiometric sensing platform to address these existing issues for the detection of heavy metals under real complex environmental and clinical conditions.

Deoxyribonucleic acid (DNA) and aptamers, as bioreceptors with high specificity, has been applied to build a variety of powerful sensing platforms [17,18]. The accelerated progress in solid-state potentiometric sensing technology has led to new potentiometric systems that utilize DNA or aptamers to detect various targets, such as butyrylcholinesterase, cardiac troponin complex and bisphenol A [19–21]. Aptamer-based sensing relies on the charge changes from the interaction of negatively charged DNA or aptamers with targets. However, most of the reported studies are based on the sensing of macromolecules, and the current development of aptasensor-based potentiometric detection of heavy-metal ionic species are still lacking. In particular, no potentiometric aptasensor for Pb^{2+} detection have been reported. Compared to macromolecules, heavy metal ionic species lacks satisfactory sensitivity and detection limits in potentiometric aptamer sensor systems as targets due to its relatively smaller molecular size. Therefore, a new potentiometric platform is essential for the potentiometric detection of ionic species.

As an emerging new strategy, the special skeletal transformation of guanine quartet to G-quadruplex (G4) structures in the presence of specific metal ions offers a new way for heavy metal detection. DNA sensors for Pb^{2+} detection have been designed based on the Pb^{2+} -induced G-quadruplex formation [22–24]. Despite their excellent sensitivity and selectivity, these DNA sensors require electrochemical labels or fluorophores for signaling, which involves complex fabrication and detection process. Unlike these reported approaches, potentiometric aptasensors based on the change on surface-charge density can simply provide response signals without the use of any labels [25]. Hence, it is highly desirable to develop a highly specific aptasensor using simple and low-power potentiometric detection systems for the detection of Pb^{2+} in complex biological or environmental samples.

Herein, we report for the first time, a label-free potentiometric aptasensor for the detection of Pb^{2+} (Scheme 1). Based on the specific binding between DNA strands and Pb^{2+} ions that transforms DNA strands into stable G4 structures, a “sandwich-type” detection strategy with highly selective sensing mechanism can be established. In addition, polyion oligonucleotide-labeled gold nanoparticles (AuNPs-DNA), as signal-amplified probes to enhance the output electrical signal and control the interfacial amount of DNA, are used to modify the Au electrode to provide high-density negative charges on the electrode surface [26]. Gold dendritic (DenAu) with three-dimensional nanostructures and high surface areas were employed as the solid contact to maximize the immobilization of aptasensor, ensure optimum signal, and decrease the resistance of the potentiometric sensing platform. The developed

aptasensors were also successfully implemented in the detection of real samples. The demonstrated potentiometric aptamer-based sensor with high selectivity offers a promising future for the on-site detection of heavy-metal species.

2. Experimental section

2.1. Reagents and materials

Tetrachloroaurate (III) tetrahydrate ($\text{HAuCl}_4 \cdot 4\text{H}_2\text{O}$, 47.8% Au) was purchased from Tokyo Chemical Industry Co., Ltd. (Tokyo, Japan). KCl, Na_2HPO_4 , NaH_2PO_4 , hydrogen peroxide (30%), CaCl_2 , $\text{Cu}(\text{NO}_3)_2$, $\text{Hg}(\text{NO}_3)_2$, ZnCl_2 , NiCl_2 , FeCl_3 , MgCl_2 and $\text{Pb}(\text{NO}_3)_2$ were obtained from Sinopharm Chemical Reagent Co., LTD. (Shanghai, China). Cd (II) standard solution (1 mg mL^{-1}) was purchased from Merck Serono Co., Ltd. (Shanghai, China). Sulfuric acid (99.99%), DNA sequences were synthesized by Shanghai Sangon Biological Engineering Technology & Service Co. Ltd. (Shanghai, China). Gold nanoparticles (30 nm, stabilized suspension in citrate buffer) were purchased from Sigma-Aldrich. The tap water, lake water and river water samples were collected from our lab, the lake of Binjiang Park (Shanghai, China) and Huangpu River (Shanghai, China), respectively. All other chemicals were of analytical grade and used without further purification. Doubly distilled water ($\geq 18 \text{ M}\Omega \text{ cm}$), generated by Millipore water purification system, was used throughout the experiments.

2.1.1. Sequence information

C₁-DNA: HS-CACCCTCCAC- 3'

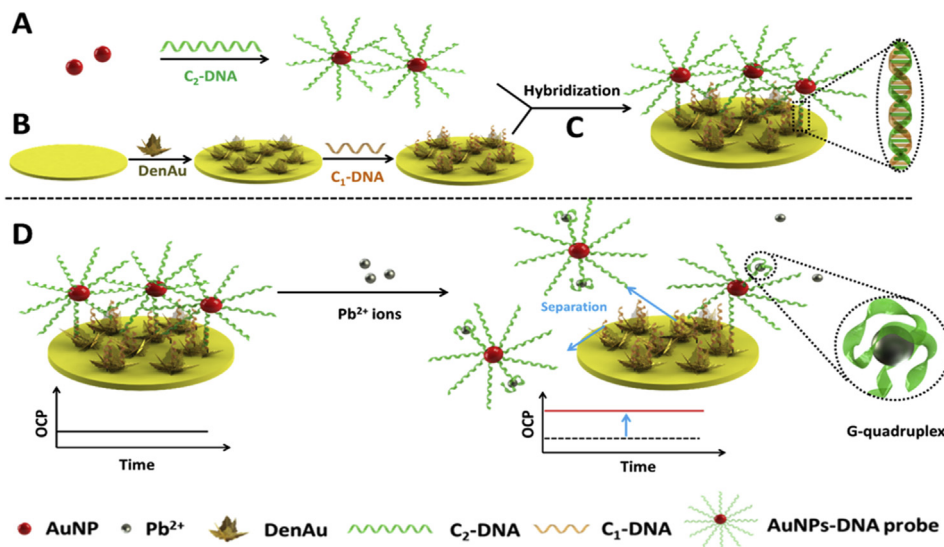
C₂- DNA: HS-GGGTGGGTGGGTGGGTGGGT- 5'

2.2. Apparatus and measurements

Open circuit potential (OCP) measurements were carried out with a CHI660C electrochemical workstation (CH Instruments, Shanghai, China). The pH values of series of 0.1 M PBS (containing Na_2HPO_4 – NaH_2PO_4 and NaCl) were measured by a PHS-3C pH meter (Leici Instrumental Corporation, Shanghai, China). All potentials reported in this paper are referenced to the Ag/AgCl reference electrodes (filled with 3.0 M KCl). OCP detection was investigated with a two-electrode system, comprising of the modified Au electrode as the indicating electrode and Ag/AgCl as the reference electrode. Morphologies of the modified electrode surfaces were observed with scanning electronic microscopy (Hitachi S-4800 equipped with EDX detector). The solid-state UV spectra were collected by UV/vis/NIR spectrophotometer (Lambda 950, PerkinElmer, USA). The determination of real samples was verified by inductively coupled plasma mass spectrometry (ICP-MS, Element 2, Thermo Finnigan, Germany).

2.3. Preparation of DenAu

The Au electrodes (0.04 cm^2) were rinsed thoroughly with piranha solution (the mixtures of concentrated sulfuric acid and hydrogen peroxide with the volume ratio of 7:3), followed by cleaning in ethanol and water for 5 min consecutively with ultrasonication. The electrode was then polished with 0.05 and 0.3 μm alumina slurry to a mirror-like finish on chamois leather and then rinsed with double-distilled water. Subsequently, the Au electrode was electrochemically cleaned using several potential cycling between -0.2 and 1.6 V in $0.5 \text{ M H}_2\text{SO}_4$ and dried with a stream of highly purified N_2 [27]. For preparation of the DenAu, the cleaned Au electrode was immersed into a mixed 3.0 mM HAuCl_4 and $0.1 \text{ M H}_2\text{SO}_4$ aqueous solution (without stirring or N_2 bubbling) at room temperature, followed by electrodeposition at -1.5 V for 300 s in a static ambient condition [28].



Scheme 1. Schematic illustration for electrochemical biosensing system constructed by aptasensor/DenAu/Au for Pb^{2+} detection: (A) synthesis of the AuNPs-DNA probe, (B) fabrication process of the C_1 -DNA/DenAu/Au, (C) fabrication process of the Aptasensor/DenAu/Au, (D) potentiometric detection of Pb^{2+} .

2.4. Construction of the sensing platform

Initially, AuNPs were immersed into the homogeneous thiol-terminated C_2 -DNA for 12 h at 37°C (1:2 v/v ratio of AuNPs: DNA sequences), allowing assembly of thiol-terminated C_2 -DNA on the surface of AuNPs. The resulting AuNPs-DNA probes (Scheme 1A) were stored at 4°C before use. Then, C_1 -DNA/DenAu/Au was prepared by self-assembled monolayers of thiol-terminated C_1 -DNA on the gold surface of the DenAu modified Au electrode. This assembly was carried out by incubating the electrode in C_1 -DNA solution for 12 h, followed by washing with buffer (Scheme 1B). Finally, the AuNPs-DNA probes were self-assembled onto the working area via complementary base-pairing hybridization between C_1 -DNA and AuNPs-DNA for 6 h at 37°C (Scheme 1C). All the unbound thiol-terminated C_1 -DNA, AuNPs-DNA probes were washed with buffer and dried at room temperature. The modified aptasensor/DenAu/Au electrode was stored at 4°C until use.

2.5. Potentiometric detection of Pb^{2+}

As shown in Scheme 1D, the resulting electrode was incubated with the different concentrations of Pb^{2+} in PBS (pH 7.4) for 30 min at room temperature, followed by washing with 0.1 M PBS (pH 7.4). Afterward, the OCP was measured in 0.1 M PBS (pH 7.4) at room temperature. In order to evaluate the influence of nonspecific adsorption, the response of each aptasensor was continuously monitored for 100 s to obtain a stable signal before the potentials were recorded. The ΔOCP values of the aptasensors were calculated according to the following equation: $\Delta\text{OCP} = \text{OCP}_a - \text{OCP}_b$, where OCP_a and OCP_b represent the potentials after and before the electrode interacting with the Pb^{2+} for 30 min, respectively. The obtained OCP signal was registered as the sensing signal introduced by the different concentration of target Pb^{2+} .

3. Results and discussion

3.1. Principle of sensing Pb^{2+} by potentiometric aptasensing platform

The proposed potentiometric platform did not follow the Nernstian response, which used large number of negative charges

based aptamer as specificity recognition receptor instead of being entrapped in a polymeric membrane. During the affinity process, the modified AuNPs-DNA probes in direct bind to Pb^{2+} and form G4 conformations, and thus the surface charge of modified electrode was largely reduced, inducing the change of potentiometric signals, which was correlated to the concentrations of Pb^{2+} [15]. Such potential changes during sensing the Pb^{2+} target could induce by two mechanisms: (1) The bonding of C_2 -DNA with Pb^{2+} target that develops stable G4 structures that detaches from the C_1 -DNA (immobilized Au electrode). It should be noted that these leaving AuNPs-DNA probes are C_2 -DNA-based which possess negative charges. Therefore, this process decreases the degree of negative charges and increases the electrical potential at the surface of the electrode. (2) The association of C_2 -DNA target with Pb^{2+} ions that generates G4 structures without detaching from C_1 -DNA. Such association can also increase the potential on the electrode surface. Remarkably, both synergistic mechanisms could increase the OCP values and enhance the response signals. The clear change in potential difference of the modified electrode against the reference electrode before and after interacting with the target Pb^{2+} can be measured via potentiometry successfully. However, the sensing mechanism is not the same as the phase-boundary potential model in ISEs and the calibration curves do not follow the classical Nernstian model [15].

3.2. Characterization of the aptasensor

The morphological and material proprieties of aptasensor/DenAu were characterized by a scanning electron microscope equipped with energy-dispersive X-ray spectroscopy (SEM-EDX) and UV-vis spectrometer. As shown in Fig. 1A, the SEM image of aptasensor/DenAu indicates that a large amount of dendritic structures, with average diameters around 800 nm, and the lengths less than $2\ \mu\text{m}$ (Fig. S1).

To modify the sensor, a large amount AuNPs-DNA probes were immobilized on the surface of the sensor. As shown in the EDX of elemental mapping of aptasensor/DenAu, the elements gold (Au) (Fig. 1B), sulfur (S) (Fig. 1C), and phosphorous (P) (Fig. 1D) are homogeneously and uniformly dispersed on the surface, demonstrating the successful modification of a large number of aptasensor. In addition, a typical EDX spectrum (Fig. S2) of

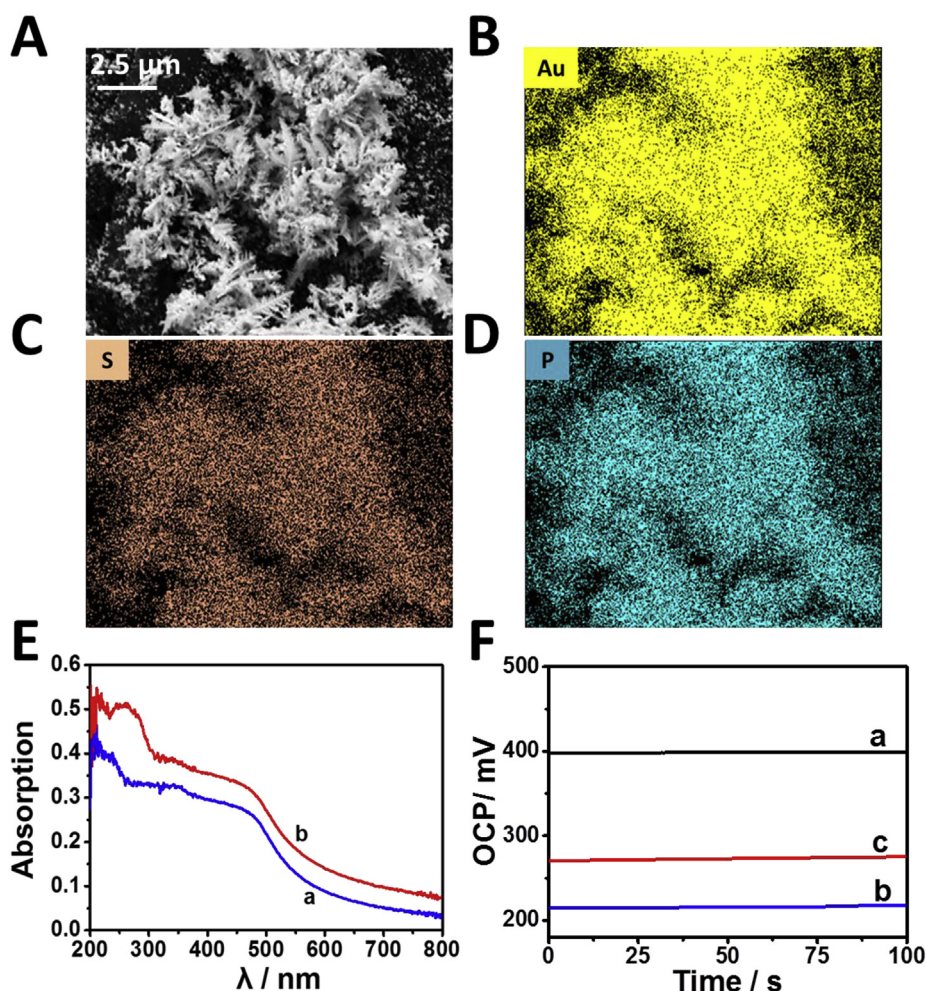


Fig. 1. (A) SEM image of aptasensor/DenAu, and energy dispersive X-ray (EDX) elemental mapping of (B) Au, (C) S, and (D) P elements of aptasensor/DenAu. (E) Solid UV–vis spectra of (a) DenAu and (b) aptasensor modified DenAu. (F) OCP curves of different modified electrodes: (a) DenAu/Au, (b) aptasensor/DenAu/Au, (c) $0.1 \mu\text{M Pb}^{2+}$ /aptasensor/DenAu/Au.

aptasensor/DenAu was also used to indicate the elemental constitution of the scanned area.

Furthermore, solid UV–vis absorption spectroscopy was used to characterize DenAu and the aptasensor. As shown in Fig. 1E, one characteristic peak at around 500 nm was observed, which indicates that the densely packed dendritic structures are symmetrically distributed on the electrode surface (curve a). As shown in curve b, two characteristics at around 260 and 500 nm for the as-prepared DenAu and aptasensors were observed. The absorption peak at around 500 nm is derived from DenAu, indicating the successful decoration of DenAu on the surface of the Au electrode. The characteristic peak at 260 nm corresponds to the C₁-DNA sequence and AuNPs-DNA probes. Overall, the obtained UV–vis spectrum confirms the successful modification of aptasensor with DenAu.

To analyze the performance of the prepared sensor in the detection of the target analyte, the aptasensor/DenAu probes were used for qualitative monitoring of $0.1 \mu\text{M Pb}^{2+}$ (as an example). As seen from Fig. 1F, initially, the OCP of DenAu modified Au electrode (DenAu/Au) was recorded (curve a). After the self-assembly of aptasensor on the DenAu/Au, a significant decrease in the OCP value (curve b) is observed which corresponds to the successful modification of negative charged aptasensor. Thereafter, the aptasensor/DenAu/Au is incubated in $0.1 \mu\text{M Pb}^{2+}$ solution. Due to the strong and specific interaction between the aptasensor and the

target Pb^{2+} , the aptasensors left from the surface of the electrodes and a dramatic increase in the OCP value is observed (curve c).

3.3. Optimization of experimental conditions

In order to optimize the detection sensitivity of the designed sensor, two variables were investigated systematically: (1) interaction time between the potentiometric sensor and the Pb^{2+} target and (2) pH of the detection solution. These effects are shown in Fig. 2. For the evaluation of the ΔOCP signal, 1.0 nM Pb^{2+} solution was utilized in all cases.

The capture and interaction between aptasensor and Pb^{2+} are strongly time-dependent. During the incubation period, there was a competitive reaction between Pb^{2+} and C₁-DNA with C₂-DNA. C₂-DNA was detached from C₁-DNA and associated with Pb^{2+} , developing stable G-quadruplex structures, which required time [29–31]. To obtain optimal ΔOCP signals, the effects of the incubation time between aptasensor and Pb^{2+} were hence investigated. As indicated in Fig. 2A, the Pb^{2+} signal increased with the increasing incubation time and stabilized after 30 min. The ΔOCP signal does not change significantly for the interaction time beyond 30 min, indicating that the interaction between aptasensor and Pb^{2+} have reached a dynamic equilibrium after 30 min. As a result, 30 min was determined as the optimum incubation time for the detection of target Pb^{2+} in our work.

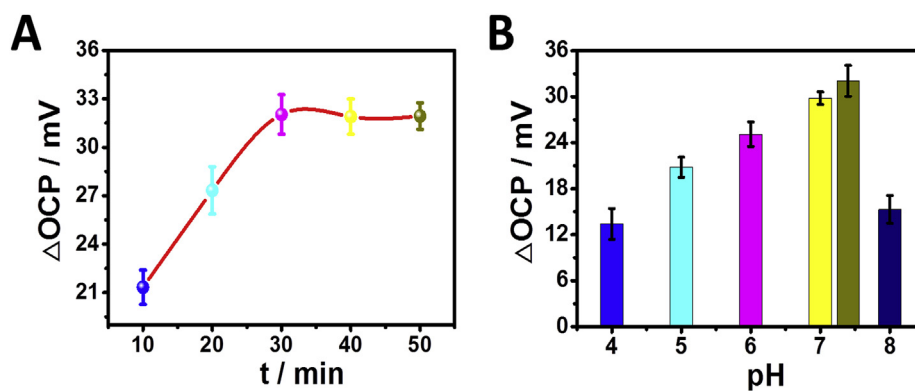


Fig. 2. Effect of (A) interaction time between the potentiometric aptasensor and target Pb^{2+} , and (B) pH value of detection solution on the ΔOCP responses of the aptasensor. All the measurements were performed in 1.0 nM Pb^{2+} solution.

Furthermore, the influence of the pH of the detection solution was investigated. The pH of detection solution influences on the interaction affinity between aptasensor and Pb^{2+} and charge intensity, therefore, is considered a crucial to the detection of Pb^{2+} . As shown in Fig. 2B, the ΔOCP signal of Pb^{2+} increased with the increase of pH value from 4.0 to 7.4 and decreased as pH increase above 7.4. This suggests that the highly acidic or alkaline surroundings may destroy the activity and special recognition ability between immobilized aptasensor and Pb^{2+} . Hence, a pH of 7.4 is selected as the optimal pH of the incubation and detection solution to obtain the maximum ΔOCP signal.

3.4. Quantitative analysis of Pb^{2+}

Under the optimal conditions, target Pb^{2+} with different concentrations were analyzed by the developed aptamer sensing platform. As reported, the solubility of Pb^{2+} can be influenced by phosphates [32], especially for Pb^{2+} with high concentration; therefore, we found that this sensing platform shows a linear relationship from the range of 10^{-11} to 10^{-6} M as illustrated in Fig. 3A with a regression coefficient (R^2) of 0.9980. The equation of the curve was calculated to be $\Delta\text{OCP} = 13.03 \lg(C_{\text{Pb}^{2+}}) + 150.24$, where $C_{\text{Pb}^{2+}}$ corresponds to the concentration of Pb^{2+} ions (M). Notably, the calibration curve displays the good linear relationship between the ΔOCP values and logarithm of the analyte concentrations with a low detection limit (LOD) of 8.5 pM ($S/N = 3$). The results indicate that the developed sensing platform for the detection of the Pb^{2+} target has a wide linear range and improved

sensitivity compared with our previous work [25]. As discussed in reported works [15,21,25,33,34], the variation of ΔOCP values was influenced by the variation of the negative charged AuNPs-DNA-probe-based sensing platform during the recognition event, indicating that the potentiometric measurements did not follow the Nernstian response. A comparison of the analytical performance of aptasensor/DenAu in this work and other reports is shown in Table 1. The detection limit in this proposed method was comparable to other work, and the modification process was relatively simple compared with the Pb^{2+} biosensors with labels [35–41].

In order to evaluate the selectivity of the aptasensor based on C1-DNA and AuNPs-DNA probes, the voltage responses toward the

Table 1
Analytical performance comparison between different Pb^{2+} biosensors.

Detection method	Probe	Detection limit	Reference
RRS	TBA	900 pM	[35]
Colorimetry	DNAzyme and MB	20.0 pM	[36]
DPV	(Fe–P)n-MOF-Au-GR	20.0 pM	[37]
Chronocoulometry	DNAzyme and RuHex	12.0 pM	[38]
Photoelectrochemical	AuNP-labeled DNA	50.0 pM	[39]
SWASV	PANI NTs	96.5 pM	[40]
Potentiometry	PANI microfibers	630 pM	[41]
Potentiometry	Aptasensor	8.50 pM	This work

Abbreviations. RRS: resonance Rayleigh scattering. TBA: thrombin binding aptamer. MB: molecular beacon. DPV: differential pulse voltammetry. (Fe–P)n-MOF-Au-GR: DNA functionalized iron-porphyrinic metal-organic framework. RuHex: hexaammineruthenium (III) chloride. PANI NTs: Size-tunable polyaniline nanotubes. PANI: Electrospun polyaniline.

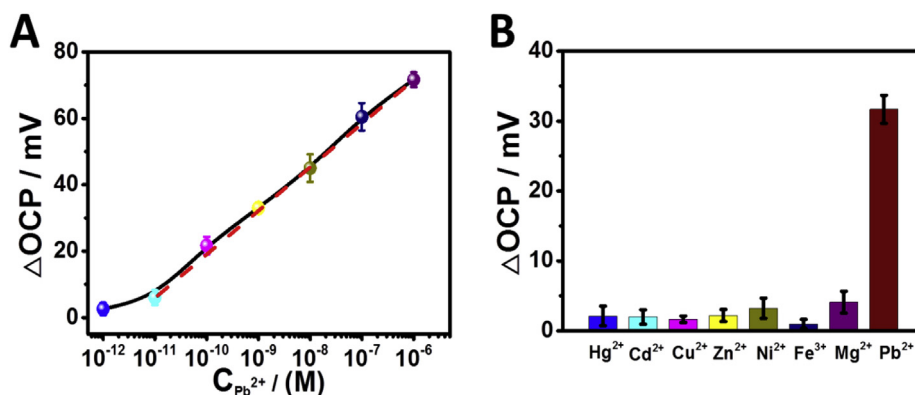


Fig. 3. (A) Calibration curve of aptasensor/DenAu/Au obtained from the sensing platform versus the logarithm of Pb^{2+} in PBS (pH 7.4) solution concentrations. (B) Selectivity of the potentiometric aptasensors array against $1.0 \mu\text{M}$ interfering ions added in PBS (pH 7.4) solution.

Table 2
Detection of Pb^{2+} in water samples with the proposed method. ($n = 3$).

Water sample	Added (nM)	Proposed Method			ICPMS		
		Found (nM)	Apparent Recovery (%)	RSD (%)	Found (nM)	Apparent Recovery (%)	RSD (%)
Tap water	5.0	5.01	100.2	4.54	4.79	95.8	1.11
	10.0	9.77	97.7	4.18	10.15	101.5	1.33
Lake water	5.0	5.13	102.6	2.58	5.38	107.6	2.66
	10.0	10.23	102.3	4.48	10.32	103.2	1.84
River water	5.0	4.87	97.4	3.78	5.21	104.2	1.30
	10.0	10.47	104.7	3.17	10.19	101.9	2.76

Pb^{2+} analyte and a variety of potential interferences were evaluated. Samples that contains various metal ions expected to co-exist in the real-life situation, namely, $1.0 \mu M Hg^{2+}$, Cd^{2+} , Cu^{2+} , Zn^{2+} , Ni^{2+} , Fe^{3+} , and Mg^{2+} were investigated. As illustrated in Fig. 3B, the $1.0 nM Pb^{2+}$ displays a notable increase in the ΔOCP signal, compare to the solutions containing other interfering ions, suggesting high and favorable selectivity of the developed platform. These data illustrate that the presence of other complex non-target pollutants in the environment does not interfere with the Pb^{2+} detection. Consequently, the constructed sensing system is considered highly selective, enabling the applicable detection of Pb^{2+} in real complex media.

Moreover, the repeatability and stability of aptasensor-based sensing platform was also investigated. The repeatability was studied by detecting $0.1 nM$ and $1.0 nM Pb^{2+}$ in PBS (pH 7.4), respectively. The obtained relative standard deviations (RSDs) are 3.23% and 4.98%, respectively, showing that the sensing system had satisfactory repeatability (Fig. S3). The stability was investigated at $1.0 nM Pb^{2+}$, and the results show that the sensing platform has no obvious decay after the modified electrodes were stored at $4^\circ C$ for 7 days (Fig. S4).

3.5. Detection of Pb^{2+} in real samples

To evaluate the applicability of the aptasensor-based potentiometric sensing system, different water samples, including tap, lake, and river water were analyzed. The detailed procedures are shown in the Supporting Information. As presented in Table 2, a significant increase in OCP value was observed, with the increment of spiked Pb^{2+} concentration at 5.0 and 10.0 nM. Table 2 shows an apparent recovery in the range of 97.4%–104.7% with acceptable RSDs. Moreover, the results achieved from this work great well with the results from ICPMS, suggesting that our designed sensing system could be applied for the detection of target Pb^{2+} in the environmental monitoring.

4. Conclusion

This article describes, for the first time, a label-free aptasensor-based potentiometric sensor, with the specially structured large surface area and high capacity charge storage based high-double-layer-capacitance DenAu as the solid conduct layer, for the stable and reliable detection of Pb^{2+} . The sensing platform displays favorable reproducibility with prolonged service life. The sensitive ΔOCP response toward the Pb^{2+} target yielded good linearity over the wide range of 10^{-11} to $10^{-6} M$ with the detection limit as low as $8.5 pM$. Compared with other traditional electrochemical detection strategies, the present aptasensor based potentiometric sensing system presented higher selectivity for the detection of Pb^{2+} in environmental conditions. In addition, the sensor gave outstanding performance to directly detect the heavy metal without sophisticated processes, which opens up a promising new horizon in

potentiometric sensing applications for environment monitoring. This proposed system awaits further improvement toward real-life application. Future works can include the integration with portable device or wearable electronics for user-friendly and wide application in on-site detection and warning system.

Declaration of interests

The authors declare that they have no known competing financial interests or personal relationships that could have appeared to influence the work reported in this paper.

Acknowledgements

This work was financially supported by the National Natural Science Foundation of China (Grant No. 21575042). W. Tang acknowledges the support from the China Scholarship Council (CSC).

Appendix A. Supplementary data

Supplementary data to this article can be found online at <https://doi.org/10.1016/j.aca.2019.06.020>.

References

- [1] P. Bühlmann, E. Pretsch, E. Bakker, Carrier-based ion-selective electrodes and bulk optodes. 2. ionophores for potentiometric and optical sensors, *Chem. Rev.* 98 (1998) 1593–1688.
- [2] G.A. Crespo, Recent advances in Ion-selective membrane electrodes for in situ environmental water analysis, *Electrochim. Acta* 245 (2017) 1023–1034.
- [3] E. Woźnica, M.M. Wójcik, M. Wojciechowski, J. Mieczkowski, E. Bulska, K. Maksymiuk, A. Michalska, Dithizone modified gold nanoparticles films for potentiometric sensing, *Anal. Chem.* 84 (2012) 4437–4442.
- [4] J. Sutter, A. Radu, S. Peper, E. Bakker, E. Pretsch, Solid-contact polymeric membrane electrodes with detection limits in the subnanomolar range, *Anal. Chim. Acta* 523 (2004) 53–59.
- [5] J.H. Li, T.J. Yin, W. Qin, An effective solid contact for an all-solid-state polymeric membrane Cd^{2+} -selective electrode: three-dimensional porous graphene-mesoporous platinum nanoparticle composite, *Sensor. Actuator. B* 239 (2017) 438–446.
- [6] J.B. Hu, A. Stein, P. Bühlmann, Rational design of all-solid-state ion-selective electrodes and reference electrodes, *Trends Anal. Chem.* 76 (2016) 102–114.
- [7] J. Bobacka, Potential stability of all-solid-state ion-selective electrodes using conducting polymers as ion-to-electron transducers, *Anal. Chem.* 71 (1999) 4932–4937.
- [8] L. Mendecki, T. Fayose, K.A. Stockmal, J. Wei, S. Granados-Focil, C.M. McGraw, A. Radu, Robust and ultrasensitive polymer membrane-based carbonate-selective electrodes, *Anal. Chem.* 87 (2015) 7515–7518.
- [9] H.N. Kim, W.X. Ren, J.S. Kim, J. Yoon, Fluorescent and colorimetric sensors for detection of lead, cadmium, and mercury ions, *Chem. Soc. Rev.* 41 (2012) 3210–3244.
- [10] M.R. Saidur, A.R. Abdul Aziz, W.J. Basirun, Recent advances in DNA-based electrochemical biosensors for heavy metal ion detection: a review, *Biosens. Bioelectron.* 69 (2015) 230–234.
- [11] V.K. Gupta, M.A. Khayat, A.K. Singh, M.K. Pal, Nano level detection of Cd(II) using poly(vinyl chloride) based membranes of Schiff bases, *Anal. Chim. Acta* 634 (2009) 36–43.
- [12] A. Ceresa, A. Radu, S. Peper, E. Bakker, E. Pretsch, Rational design of potentiometric trace level ion sensors. A Ag^{+} -Selective electrode with a 100 ppt detection limit, *Anal. Chem.* 74 (2002) 4027–4036.

- [13] M. Lerchi, E. Bakker, B. Rusterholz, W. Simon, Lead-selective bulk optodes based on neutral ionophores with subnanomolar detection limits, *Anal. Chem.* 64 (1992) 1534–1540.
- [14] A. Michalska, J. Dumańska, K. Maksymiuk, Lowering the detection limit of ion-selective plastic membrane electrodes with conducting polymer solid contact and conducting polymer potentiometric sensors, *Anal. Chem.* 75 (2003) 4964–4974.
- [15] A. Düzgün, G.A. Zelada-Guillén, G.A. Crespo, S. Macho, J. Riu, F.X. Rius, Nanostructured materials in potentiometry, *Anal. Bioanal. Chem.* 399 (2011) 171–181.
- [16] H. Zhang, R. Yao, N. Wang, R.N. Liang, W. Qin, Soluble molecularly imprinted polymer-based potentiometric sensor for determination of bisphenol AF, *Anal. Chem.* 90 (2008) 657–662.
- [17] J.B. Zhu, L.B. Zhang, Z.X. Zhu, S.J. Dong, E.K. Wang, Aptamer-based sensing platform using three-way DNA junction-driven strand displacement and its application in DNA logic circuit, *Anal. Chem.* 86 (2014) 312–316.
- [18] H. Pei, N. Lu, Y.L. Wen, S.P. Song, Y. Liu, H. Yan, C.H. Fan, A DNA nanostructure-based biomolecular probe carrier platform for electrochemical biosensing, *Adv. Mater.* 22 (2010) 4754–4758.
- [19] J.W. Ding, B.W. Li, L.X. Chen, W. Qin, A three-dimensional origami paper-based device for potentiometric biosensing, *Angew. Chem. Int. Ed.* 55 (2016) 13033–13037.
- [20] Q. Zhang, A. Prabhu, A. San, J.F. Al-Sharab, K. Levon, A polyaniline based ultrasensitive potentiometric immunosensor for cardiac troponin complex detection, *Biosens. Bioelectron.* 72 (2015) 100–106.
- [21] J.W. Ding, Y. Gu, F. Li, H.X. Zhang, W. Qin, DNA nanostructure-based magnetic beads for potentiometric aptasensing, *Anal. Chem.* 87 (2015) 6465–6469.
- [22] B. Zhang, J.F. Chen, B.Q. Liu, D.P. Tang, Amplified electrochemical sensing of lead ion based on DNA-mediated self-assembly-catalyzed polymerization, *Biosens. Bioelectron.* 69 (2015) 230–234.
- [23] T. Li, S.J. Dong, E.K. Wang, A lead (II)-driven DNA molecular device for turn-on fluorescence detection of lead (II) ion with high selectivity and sensitivity, *J. Am. Chem. Soc.* 132 (2010) 13156–13157.
- [24] F. Li, Y. Feng, C. Zhao, B. Tang, Crystal violet as a G-quadruplex-selective probe for sensitive amperometric sensing of lead, *Chem. Commun.* 47 (2011) 11909–11911.
- [25] W.X. Tang, Z.Z. Wang, J. Yu, F. Zhang, P.G. He, Internal calibration potentiometric aptasensors for simultaneous detection of Hg^{2+} , Cd^{2+} , and As^{3+} based on screen-printed carbon electrodes array, *Anal. Chem.* 90 (2018) 8337–8344.
- [26] J. Zhang, S.P. Song, L.Y. Zhang, L.H. Wang, H.P. Wu, D. Pan, C.H. Fan, Sequence-specific detection of femtomolar DNA via a chronocoulometric DNA sensor (CDS): effects of nanoparticle-mediated amplification and nanoscale control of DNA assembly at electrodes, *J. Am. Chem. Soc.* 128 (2006) 8575–8580.
- [27] S. Yang, L.J. Liu, M. You, F. Zhang, X.J. Liao, P.G. He, The novel pillar[5]arene derivative for recyclable electrochemical sensing platform of homogeneous DNA hybridization, *Sensor. Actuator. B Chem.* 227 (2016) 497–503.
- [28] F. Li, X.P. Han, S.F. Liu, Development of an electrochemical DNA biosensor with a high sensitivity of fM by dendritic gold nanostructure modified electrode, *Biosens. Bioelectron.* 26 (2011) 2619–2625.
- [29] L.Q. Guo, D.D. Nie, C.Y. Qiu, Q.S. Zheng, H.Y. Wu, P.R. Ye, Y.L. Hao, F.F. Fu, G.N. Chen, A G-quadruplex based label-free fluorescent biosensor for lead ion, *Biosens. Bioelectron.* 35 (2012) 123–127.
- [30] F. Li, Y. Feng, C. Zhao, B. Tang, Crystal violet as a G-quadruplex-selective probe for sensitive amperometric sensing of lead, *Chem. Commun.* 47 (2011) 11909–11911.
- [31] T. Li, E.K. Wang, S.J. Dong, Lead(II)-Induced allosteric G-quadruplex DNzyme as a colorimetric and chemiluminescence sensor for highly sensitive and selective Pb^{2+} detection, *Anal. Chem.* 82 (2010) 1515–1520.
- [32] S. Sauvé, M. McBride, Lead phosphate solubility in water and soil suspensions, *Environ. Sci. Technol.* 32 (1998) 388–393.
- [33] G.A. Zelada-Guillén, J. Riu, A. Düzgün, F. Xavier Rius, Immediate detection of living bacteria at ultralow concentrations using a carbon nanotube based potentiometric aptasensor, *Angew. Chem. Int. Ed.* 48 (2009) 7334–7337.
- [34] Y. Zhou, B. Yu, A. Guiseppi-Elie, V. Sergeev, K. Levon, Potentiometric monitoring DNA hybridization, *Biosens. Bioelectron.* 24 (2009) 3275–3280.
- [35] X.B. Fu, F. Qu, N.B. Li, Q. Luo, A label-free thrombin binding aptamer as a probe for highly sensitive and selective detection of lead(II) ions by a resonance Rayleigh scattering method, *Analyst* 137 (2012) 1097–1099.
- [36] W. Yun, D.Z. Cai, J.L. Jiang, P.X. Zhao, Y. Huang, G. Sang, Enzyme-free and label-free ultra-sensitive colorimetric detection of Pb^{2+} using molecular beacon and DNzyme based amplification strategy, *Biosens. Bioelectron.* 80 (2016) 187–193.
- [37] X. Wang, C.L. Yang, S.J. Zhu, M. Yan, S.G. Ge, J.H. Yu, 3D origami electrochemical device for sensitive Pb^{2+} testing based on DNA functionalized iron-porphyrinic metal-organic framework, *Biosens. Bioelectron.* 87 (2017) 108–115.
- [38] C. Zhang, C. Lai, G.G. Zeng, D.L. Huang, L. Tang, C.P. Yang, Y.Y. Zhou, L. Qin, M. Cheng, Nanoporous Au-based chronocoulometric aptasensor for amplified detection of Pb^{2+} using DNzyme modified with Au nanoparticles, *Biosens. Bioelectron.* 81 (2016) 61–67.
- [39] Y. Zang, J.P. Lei, Q. Hao, H.X. Ju, “Signal-on” photoelectrochemical sensing strategy based on target-dependent aptamer conformational conversion for selective detection of lead (II) ion, *ACS Appl. Mater. Interfaces* 6 (2014) 15991–15997.
- [40] G.D. Zhu, Y.X. Ge, Y. Dai, X.H. Shang, J.M. Yang, J.Y. Liu, Size-tunable polyaniline nanotube-modified electrode for simultaneous determination of Pb(II) and Cd(II), *Electrochim. Acta* 268 (2018) 202–210.
- [41] C.C. Liu, X.H. Jiang, Y.Y. Zhao, W.W. Jiang, Z.M. Zhang, L.M. Yu, A solid-contact Pb^{2+} -selective electrode based on electrospun polyaniline microfibers film as ion-to-electron transducer, *Electrochim. Acta* 231 (2017) 53–60.